Kinetics of the Reactions of Cl*($^2P_{1/2}$) and Cl($^2P_{3/2}$) Atoms with CH_3OH, C_2H_5OH, *n*-C_3H_7OH, and *i*-C_3H_7OH at 295 K

Fumikazu Taketani, Kenshi Takahashi, and Yutaka Matsumi*

Solar-Terrestrial Environment Laboratory and Graduate School of Science, Nagoya University, Honohara 3-13, Toyokawa, Aichi, 442-8507 Japan

Timothy J. Wallington

Physical and Environmental Sciences Department, Ford Motor Company, SRL-3083, Dearborn, Michigan 48121-2053

Received: January 5, 2005; In Final Form: February 10, 2005

The title reactions were studied using laser flash photolysis/laser-induced-fluorescence (FP-LIF) techniques. The two spin−orbit states, Cl*($^2P_{1/2}$) and Cl($^2P_{3/2}$), were detected using LIF at 135.2 and 134.7 nm, respectively. Measured reaction rate constants were as follows (units of cm^3 $molecule^{-1}$ s^{-1}): $k(Cl(^2P_{3/2})+CH_3OH) = (5.35 \pm 0.24) \times 10^{-11}$, $k(Cl(^2P_{3/2})+C_2H_5OH) = (9.50 \pm 0.85) \times 10^{-11}$, $k(Cl(^2P_{3/2})+n\text{-}C_3H_7OH) = (1.71 \pm 0.11) \times 10^{-10}$, and $k(Cl(^2P_{3/2})+i\text{-}C_3H_7OH) = (9.11 \pm 0.60) \times 10^{-11}$. Measured rate constants for total removal of Cl*($^2P_{1/2}$) in collisions with CH_3OH, C_2H_5OH, *n*-C_3H_7OH, and *i*-C_3H_7OH were $(1.95 \pm 0.13) \times 10^{-10}$, $(2.48 \pm 0.18) \times 10^{-10}$, $(3.13 \pm 0.18) \times 10^{-10}$, and $(2.84 \pm 0.16) \times 10^{-10}$, respectively; quoted errors are two-standard deviations. Although spin−orbit excited Cl*($^2P_{1/2}$) atoms have 2.52 kcal/mol more energy than Cl($^2P_{3/2}$), the rates of chemical reaction of Cl*($^2P_{1/2}$) with CH_3OH, C_2H_5OH, *n*-C_3H_7OH, and *i*-C_3H_7OH are only 60−90% of the corresponding Cl($^2P_{3/2}$) atom reactions. Under ambient conditions spin−orbit excited Cl* atoms are responsible for 0.5%, 0.5%, 0.4%, and 0.7% of the observed reactivity of thermalized Cl atoms toward CH_3OH, C_2H_5OH, *n*-C_3H_7OH, and *i*-C_3H_7OH, respectively.

1. Introduction

Atomic chlorine plays an important role in atmospheric chemistry.[1] The main atmospheric fate of Cl atoms is reaction with organic compounds and ozone. Many different kinetic techniques have been applied to study the reactions of atomic chlorine with organic compounds. For the reactions of atomic chlorine with alcohols, various experimental techniques such as discharge flow/electron paramagnetic resonance,[2] Fourier transform infrared (FT-IR)/smog chamber study (relative rate method),[3−5] discharge flow/mass spectrometric detection,[6,7] laser photolysis/chemical luminescence detection,[8] laser photolysis/resonance fluorescence detection,[9] flash photolysis/resonance fluorescence detection,[10] and laser photolysis/infrared absorption[5,8,11] have been used. As a result, there is a large kinetic database concerning such reactions at ambient temperatures.[12]

The existing kinetic database for reactions of atomic chlorine does not differentiate between the reactivity of the Cl*($^2P_{1/2}$) (denoted below as Cl*) and Cl($^2P_{3/2}$) (denoted below as Cl) states. The spin−orbit Cl* and Cl states are separated by 2.52 kcal/mol (882 cm^{-1}), and at ambient temperature there is an appreciable population of the excited Cl* state (0.71% at 298 K). The reactivity of these two spin−orbit states is expected to differ considerably. In reactions of halogen atoms, the ground spin−orbit state $^2P_{3/2}$ is generally considered to be more reactive than the $^2P_{1/2}$ state due to the adiabatic nature of the corresponding potential surfaces.[13] However, there is little information concerning the relative importance of the Cl* and Cl states in the reactions of Cl atoms with organic compounds.[14−16]

In this study, laser flash photolysis/laser-induced-fluorescence techniques have been applied to investigate the reactivity of both Cl and Cl* with methanol, ethanol, 1-propanol, and 2-propanol at 295 ± 2 K. Cl and Cl* atoms were produced by 193 nm pulsed excimer laser photolysis of HCl. The concentrations of Cl and Cl* in the presence of alcohol reactant were monitored as a function of time by vacuum UV laser-induced-fluorescence techniques. The removal processes of Cl and Cl* atoms following collision with alcohol (ROH) molecules are

$$Cl + ROH \xrightarrow{k_{reac}} HCl + (products) \quad \text{reaction of Cl} \quad (1)$$

$$Cl + ROH \xrightarrow{k_{ex}} Cl^* + ROH \quad \text{excitation of Cl} \quad (2)$$

$$Cl^* + ROH \xrightarrow{k^*_{reac}} HCl + (products) \quad \text{reaction of Cl*} \quad (3)$$

$$Cl^* + ROH \xrightarrow{k^*_{relax}} Cl + ROH \quad \text{relaxation of Cl*} \quad (4)$$

where k_{reac}, k_{ex}, k^*_{reac}, and k^*_{relax} are rate constants for processes 1−4.

Enthalpy data[17−22] for reactions of Cl atoms with CH_3OH, C_2H_5OH, *n*-C_3H_7OH, and *i*-C_3H_7OH are listed in Table 1. Figure 1 gives the schematic energy diagram for the Cl + C_2H_5OH system. The reaction paths for CH_3CHOH + HCl (α-hydrogen abstraction), CH_2CH_2OH + HCl (β-hydrogen abstraction), and CH_3CH_2O + HCl (hydroxyl hydrogen abstraction) are indicated with the energy barriers that were obtained by Rudić et al.[23] from ab initio calculations. The energy of the Cl* + ROH system is higher by 2.52 kcal mol^{-1} than that of the Cl + ROH

* Corresponding author. Fax: +81-533-89-5593. E-mail: matsumi@stelab.nagoya-u.ac.jp.

10.1021/jp050055t CCC: $30.25
Published on Web 04/02/2005

TABLE 1: Enthalpies of Reactions of Cl Atoms with CH_3OH, C_2H_5OH, *n*-C_3H_7OH, and *i*-C_3H_7OH

reactants	products	ΔH^a/kcal mol^{-1}
$CH_3OH + Cl(^2P_{3/2})$	$CH_3O + HCl$	1.2
	$CH_2OH + HCl$	−5.8
$C_2H_5OH + Cl(^2P_{3/2})$	$CH_3CH_2O + HCl$	1.4
	$CH_3CHOH + HCl$	−10.1
	$CH_2CH_2OH + HCl$	−2.6
n-$C_3H_7OH + Cl(^2P_{3/2})$	$CH_3CH_2CH_2O + HCl$	0.3
	$CH_3CH_2CHOH + HCl$	−13.5
	$CH_3CHCH_2OH + HCl$	−8.9
	$CH_2CH_2CH_2OH + HCl$	−6.1
i-$C_3H_7OH + Cl(^2P_{3/2})$	$CH_3CHOCH_3 + HCl$	0.8
	$CH_3COHCH_3 + HCl$	−11.5
	$CH_3CH(OH)CH_2 + HCl$	−8.9

[a] Reaction enthalpy.[17−22]

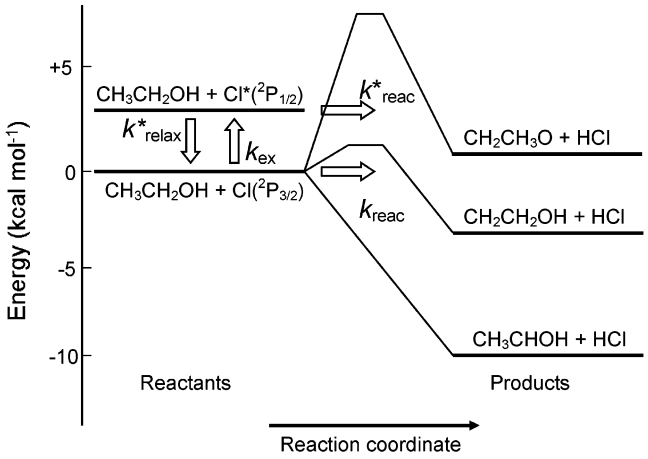

Figure 1. Schematic energy diagram for the $Cl(^2P_{3/2})/Cl^*(^2P_{1/2}) + C_2H_5OH$ system. Reaction energy barrier heights are taken from Rudić et al.[23]

system. Interestingly, in the reaction of $Cl + C_2H_5OH$, the barrier for H-atom abstraction from the β-position of C_2H_5OH was calculated to be 0.73 kcal mol^{-1} with respect to the reactants,[23] which is lower than the spin−orbit excitation energy of Cl* atom. If spin−orbit excitation were effective in overcoming the barrier for H-atom abstraction from the β-position, we would expect Cl* to have a greater reactivity than Cl atoms.

To improve our understanding of reactions of Cl atoms with organic compounds, we conducted a detailed kinetic study of the reactions of ground and spin−orbit excited chlorine atoms with a series of alcohols. Rate constants for processes 1, 3, and 4 (k_{reac}, k^*_{reac}, and k^*_{relax}) were determined and are reported herein.

2. Experimental Section

Experiments were conducted using the laser flash photolysis laser-induced-fluorescence apparatus described in detailed elsewhere.[14,15] $Cl(^2P_j)$ atoms were produced by the 193 nm photolysis of HCl, which gives 59% $Cl(^2P_{3/2})$ and 41% $Cl^*(^2P_{1/2})$.[24] An ArF excimer laser (Lambda Physik, COMPex 102) was employed as the photolysis light source.

$$HCl + h\nu\ (193\ nm) \rightarrow H + Cl(^2P_{3/2}) \qquad 59\% \qquad (5)$$

$$\rightarrow H + Cl^*(^2P_{1/2}) \qquad 41\% \qquad (6)$$

Based on the reported absorption cross section of HCl at 193 nm (8.69×10^{-20} cm^2)[25] and the photolysis laser fluence, we estimated the initial concentration of chlorine (Cl and Cl*) atoms in the present experiments to be 5×10^{11} atoms cm^{-3}. The Cl and Cl* atoms produced from the photolysis of HCl have relatively little translational excitation, since most of the excess energy goes into the translational energy of the H atom. Nevertheless, buffer gases were added to the reaction mixtures to suppress hot atom effects in the kinetic study. $Cl(^2P_{3/2})$ and $Cl^*(^2P_{1/2})$ were detected using vacuum ultraviolet laser-induced fluorescence (VUV-LIF) at 134.7 nm ($4s\ ^2P_{3/2} \rightarrow 3p\ ^2P_{3/2}$) and 135.2 nm ($4s\ ^2P_{1/2} \rightarrow 3p\ ^2P_{1/2}$), respectively. The tunable probe VUV light was generated by four-wave mixing ($2\omega_1-\omega_2$) in Kr gas using two dye lasers pumped by a single XeCl excimer laser (Lambda Physik, COMPex 201, FL3002, and Scanmate 2E). The wavelength of ω_1 was 212.56 nm, corresponding to a two-photon resonance to the Kr $5p[1/2]_0$ state. The wavelength of ω_2 was tuned near 500 nm. Typical pulse energies were 0.2 and 4 mJ for the ω_1 and ω_2 lasers, respectively. The ω_1 and ω_2 laser beams were focused into a cell containing Kr gas at 15−20 Torr with a fused silica lens ($f = 200$). The resultant VUV light beam passed through a LiF window into the reaction cell.

The VUV-LIF signal from Cl* or Cl was detected by a solar-blind photomultiplier tube (PMT; EMR, 541J-08-17) mounted at right angles to the propagation direction of the probing VUV beam and the 193 nm photolysis beam. The 193 nm laser light and the VUV laser light crossed perpendicularly in the reaction cell. The PMT has a LiF window and a KBr photocathode that is sensitive only between 105 and 150 nm. The output from the PMT was preamplified and fed into a gated integrator (Stanford Research, SR-250). The delay time between the photolysis and probe laser pulses was controlled by a pulse generator (Stanford Research, DG535), and the jitter of the delay time was less than 10 ns. Both photolysis and probe lasers were operated with the repetition rate of 10 Hz. In typical experiments, the delay time was scanned to cover the whole time domain of the fluorescence signal decay, usually $t = 0-300$ μs (with step $\Delta t = 2$ μs) for the Cl and Cl*. At each step, the signal was averaged for 10 laser shots, and the total time of the decay profile measurements was 150 s.

Two sets of experiments were performed. First, the reactivity of spin−orbit ground state Cl atoms toward CH_3OH, C_2H_5OH, *n*-C_3H_7OH, and *i*-C_3H_7OH was measured by photolysis of HCl/reactant mixtures in 3.0 Torr CF_4 diluent. CF_4 is an efficient relaxation agent for Cl* atoms with a collisional relaxation rate constant of 2.3×10^{-11} cm^3 molecule^{-1} s^{-1} at 298 K.[15,26,27] In the presence of 3.0 Torr CF_4, Cl* atoms have a lifetime of <0.5 μs with respect to relaxation to the spin−orbit ground state. To allow sufficient time for essentially complete relaxation of Cl* atoms, kinetic data for Cl-atom reactions was derived from the Cl decay at times >5 μs after the photolysis pulse. Second, the time profiles of Cl* and Cl atoms were monitored following the photolysis of HCl/reactant mixtures in 1.5 Torr Ar diluent. Argon is an inefficient relaxation agent for Cl* atoms with a relaxation rate constant of only 3.0×10^{-16} cm^3 molecule^{-1} s^{-1}.[27] By monitoring temporal profiles of Cl* and Cl atoms in the presence of Ar diluent, kinetic data were derived for the reactivity of Cl* toward the alcohols. In all experiments, the concentrations of added reactants were at least 100 times greater than the initial chlorine atom concentration. Accordingly, the loss of Cl atoms followed pseudo-first-order kinetics.

Reagents diluted in buffer gas were provided to the reaction cell using mass flow controllers (STEC, SEC-400MARK3). Pressures in the reaction cell were monitored by a capacitance manometer (Baratron 122A, 10 Torr full scale). The gases used in the experiments had the following stated purities: HCl, 99.9%; CH_3OH, 99.8%; C_2H_5OH, 99.5%; *n*-C_3H_7OH, 99.8%;

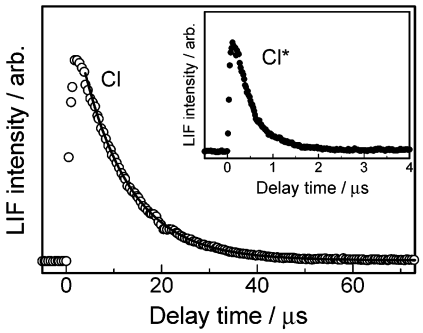

Figure 2. Decay of Cl (open circles) and Cl* (filled circles in insert) following flash photolysis of a mixture containing 6 mTorr HCl and 25.6 mTorr C_2H_5OH in 3.0 Torr CF_4 diluent at 295 ± 2 K. The solid line is a first-order-decay fit to the Cl data for times >5 μs.

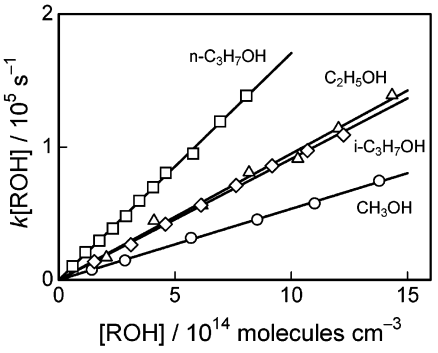

Figure 3. Pseudo-first-order loss of Cl atoms versus alcohol partial pressure: open circles, CH_3OH; open triangles, C_2H_5OH; open squares, *n*-C_3H_7OH; and open diamonds, *i*-C_3H_7OH.

i-C_3H_7OH, 99.8%; CF_4, 99.99%; and Ar, 99.999%. Alcohol samples were purified by freeze−pump−thaw cycling prior to use.

3. Results

3.1. Kinetics of Cl($^2P_{3/2}$) Atoms in Collisions with CH_3OH, C_2H_5OH, *n*-C_3H_7OH, and *i*-C_3H_7OH. Figure 2 shows the observed time profiles of the two spin−orbit states of chlorine atoms following the 193 nm pulsed irradiation of a mixture of 6.0 mTorr HCl and 25.6 mTorr C_2H_5OH in 3.0 Torr CF_4 diluent. The vertical axis scale in Figure 2 is the observed fluorescence intensity at 135.2 and 134.7 nm from Cl* and Cl, respectively, in arbitrary units. The CF_4 diluent relaxes the excited spin−orbit state Cl* to the spin−orbit ground state Cl within a few microseconds. The subsequent decay of Cl atoms at times >5 μs follows pseudo-first-order kinetics and provides information on the kinetics of the Cl + C_2H_5OH reaction. Similar experiments were performed using CH_3OH, *n*-C_3H_7OH, and *i*-C_3H_7-OH reactants.

Figure 3 shows plots of the observed pseudo-first-order decay of Cl atoms in the presence of CH_3OH, C_2H_5OH, *n*-C_3H_7OH, and *i*-C_3H_7OH reactants. The slopes of the least-squares fits give the rate constants $k_{reac}(Cl+CH_3OH) = (5.35 \pm 0.24) \times 10^{-11}$ cm^3 molecule^{-1} s^{-1}, $k_{reac}(Cl+C_2H_5OH) = (9.50 \pm 0.85) \times 10^{-11}$ cm^3 molecule^{-1} s^{-1}, $k_{reac}(Cl+n\text{-}C_3H_7OH) = (1.71 \pm 0.11) \times 10^{-10}$ cm^3 molecule^{-1} s^{-1}, and $k_{reac}(Cl+i\text{-}C_3H_7OH) = (9.11 \pm 0.60) \times 10^{-11}$ cm^3 molecule^{-1} s^{-1}. Quoted uncertainties are two standard deviations from the least-squares fits plus our estimate of systematic uncertainties associated with the reactant concentration. The rate constants for reactions of Cl with ROH obtained in the present study are listed in Table 2 together with the values reported previously.

TABLE 2: Rate Constants for Reactions of Cl($^2P_{3/2}$) with Alcohols at Room Temperature

reactant	k_{reac}[a]	method[b]	references
CH_3OH	6.15 ± 1.33	DF/EPR	Dobe et al.[2]
	5.83 ± 0.77	LP/IR	Seakins et al.[8]
	5.38 ± 0.25	LP/CL	Seakins et al.[8]
	5.6 ± 0.2	LP/IR	Smith et al.[11]
	4.57 ± 0.40	RR	Wallington et al.[3]
	6.33 ± 1.40	FP/RF	Michaela et al.[9]
	5.4 ± 0.9	LP/RF, RR	Tyndall et al.[10]
	4.79 ± 0.38	RR	Nelson et al.[4]
	5.5		IUPAC Panel[22]
	5.5		NASA/JPL Panel[25]
	5.35 ± 0.24	LP/VUV-LIF	this work
C_2H_5OH	10.2 ± 1.9	LP/CL	Seakins et al.[8]
	8.45 ± 0.91	RR	Wallington et al.[3]
	10.1 ± 0.6	RR	Nelson et al.[4]
	9.5 ± 1.9	LP/IR, RR	Taatjes et al.[5]
	10.5 ± 0.7	RR	Crawford et al.[7]
	9.6		IUPAC Panel[22]
	9.6		NASA/JPL Panel[25]
	9.50 ± 0.85	LP/VUV-LIF	this work
n-C_3H_7OH	14.4 ± 1.2	RR	Wallington et al.[3]
	14.9 ± 0.7	RR	Nelson et al.[4]
	16		IUPAC Panel[22]
	17.1 ± 1.1	LP/VUV-LIF	this work
i-C_3H_7OH	8.40 ± 0.35	RR	Nelson et al.[4]
	8.8		IUPAC Panel[22]
	9.11 ± 0.60	LP/VUV-LIF	this work

[a] Units of 10^{-11} cm^3 molecule^{-1} s^{-1}; errors are two standard deviations. [b] DF, discharge flow; EPR, electron paramagnetic resonance; LP, laser photolysis; IR, infrared absorption; CL, chemical luminescence; FP, flash photolysis; RR, relative rate; RF, resonance fluorescence; VUV-LIF, vacuum ultraviolet laser-induced fluorescence.

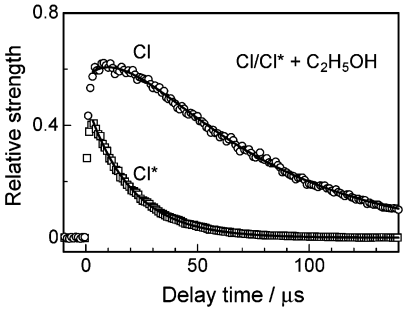

Figure 4. Time evolution of LIF signal attributable to Cl* (squares) and Cl (circles) following flash photolysis of a mixture containing 6.0 mTorr HCl and 5.6 mTorr C_2H_5OH in 1.5 Torr Ar diluent at 295 ± 2 K. The vertical scales for Cl and Cl* are adjusted to give an initial ratio [Cl]:[Cl*] = 0.59:0.41. Curves through the data were obtained using eq 11; see text for details.

3.2. Reaction and Relaxation of Cl*($^2P_{1/2}$) in Collisions with CH_3OH, C_2H_5OH, *n*-C_3H_7OH, and *i*-C_3H_7OH. To investigate the reactivity of Cl* atoms with CH_3OH, C_2H_5OH, *n*-C_3H_7OH, and *i*-C_3H_7OH, experiments were performed in 1.5 Torr Ar diluent. Argon is an inefficient quencher of Cl* atoms, and relaxation of Cl* in collisions with Ar is of negligible importance. The total removal rate constant (sum of relaxation and reaction) for Cl* in collisions with HCl is $(7.8 \pm 0.8) \times 10^{-12}$ cm^3 molecule^{-1} s^{-1}.[15] Under our experimental conditions, the pseudo-first-order rate of removal of Cl* atoms via relaxation and/or reaction process in collisions with HCl was about 1500 s^{-1} and does not make a significant contribution to Cl* loss. Figure 4 shows the observed time profiles of the two spin−orbit states following the 193 nm pulsed irradiation of a mixture of 6.0 mTorr HCl and 5.6 mTorr C_2H_5OH in 1.5 Torr Ar diluent. The relative strengths of the initial LIF signals in Figure 4 have

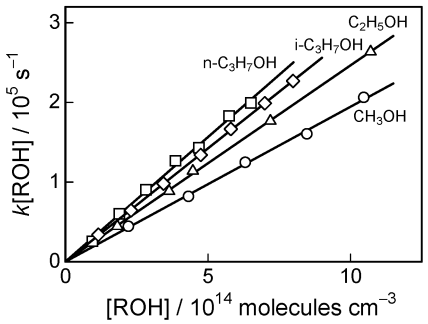

Figure 5. Pseudo-first-order loss of Cl* atoms versus alcohol partial pressure: circles, CH_3OH; triangles, C_2H_5OH; squares, *n*-C_3H_7OH; and diamonds, *i*-C_3H_7OH.

been scaled to reproduce the 0.59:0.41 ratio of Cl and Cl* formation from HCl photolysis at 193 nm.[24]

To quantify the relative importance of reactions 1−4, expressions 7 and 8 were evaluated and compared to the observed Cl and Cl* profiles.

$$\frac{d[Cl^*]}{dt} = -(k^*_{reac} + k^*_{relax})[ROH][Cl^*] + k_{ex}[ROH][Cl] \quad (7)$$

$$\frac{d[Cl]}{dt} = -(k_{reac} + k_{ex})[ROH][Cl] + k^*_{relax}[ROH][Cl^*] \quad (8)$$

The rate constant for the Cl excitation process (2) in collisions of Cl + ROH, k_{ex}, is estimated to be less than 1% that for the Cl* collisional relaxation process (4), k^*_{relax}, at 295 K based on the principle of detailed balance and energy separation of 2.52 kcal mol^{-1} between Cl* and Cl. The excitation process (2) can be neglected when [Cl*] ≫ 0.01[Cl]. The Cl* time profile is determined by loss via chemical reaction (3) and physical relaxation (4) in collisions of Cl* with ROH. Accordingly, as seen in Figure 4, the loss of Cl* follows a single-exponential form with a pseudo-first-order rate. Values for (k^*_{reac} + k^*_{relax})[ROH] were obtained from the single-exponential decay of the Cl* signal. Figure 5 shows plots of the pseudo-first-order rate of the Cl* signal versus ROH concentration. The slopes correspond to total removal (sum of reaction and relaxation) rate constants ($k^*_{total} \equiv k^*_{reac} + k^*_{relax}$) of Cl* by ROH. The values obtained are $k^*_{total}(Cl^* + CH_3OH) = (1.95 \pm 0.13) \times 10^{-10}$ cm^3 $molecule^{-1}$ s^{-1}, $k^*_{total}(Cl^* + C_2H_5OH) = (2.48 \pm 0.18) \times 10^{-10}$ cm^3 $molecule^{-1}$ s^{-1}, $k^*_{total}(Cl^* + n\text{-}C_3H_7OH) = (3.13 \pm 0.18) \times 10^{-10}$ cm^3 $molecule^{-1}$ s^{-1}, and $k^*_{total}(Cl^* + i\text{-}C_3H_7OH) = (2.84 \pm 0.16) \times 10^{-10}$ cm^3 $molecule^{-1}$ s^{-1}. Quoted errors are two standard deviations from the least-squares analyses.

The Cl profile is expected to follow either an exponential or a nonexponential profile depending on the relative magnitudes of Cl* loss processes (3) and (4). If the reactive process (3) dominates the relaxation process (4), the time profiles of Cl and Cl* will be essentially decoupled and both will follow single-exponential decay. If, on the other hand, the relaxation process (4) dominates the reactive process (3), there will be significant recovery of Cl via relaxation of Cl*, leading to a rise in the Cl time profile and hence nonexponential Cl decay.

To estimate the rate constant for reactive loss of Cl* (channel 3) in collisions with ROH, k^*_{reac}, we analyzed the observed time profiles of Cl and Cl* by an integral profiles method.[28−30]

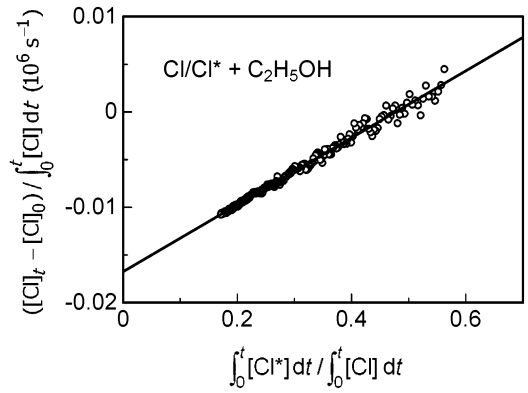

Figure 6. $([Cl]_t - [Cl]_0)/\int_0^t [Cl]_t\,dt$ versus $\int_0^t [Cl^*]_t\,dt/\int_0^t [Cl]_t\,dt$ calculated from the data in Figure 4 (see text for details).

Integration of both sides of eq 8 from $t = 0$ to t gives

$$[Cl]_t - [Cl]_0 = -(k_{reac} + k_{ex})[ROH]\int_0^t [Cl]_t\,dt + k^*_{relax}[ROH]\int_0^t [Cl^*]_t\,dt \quad (9)$$

where $[Cl]_0$ is the initial concentration of Cl after HCl photolysis at 193 nm. The left-hand side of eq 9 can be evaluated directly from the observed $[Cl]_t$ profiles as a function of delay time, *t*. Integrated values of $[Cl]_t$ and $[Cl^*]_t$ in the right-hand side of eq 9 were calculated using a trapezoidal formula. Equation 9 is rewritten as follows:

$$\frac{[Cl]_t - [Cl]_0}{\int_0^t [Cl]_t\,dt} = -(k_{reac} + k_{ex})[ROH] + k^*_{relax}[ROH]\frac{\int_0^t [Cl^*]_t\,dt}{\int_0^t [Cl]_t\,dt} \quad (10)$$

Equation 10 indicates that a plot of $([Cl]_t - [Cl]_0)/\int_0^t [Cl]_t\,dt$ versus $\int_0^t [Cl^*]_t\,dt/\int_0^t [Cl]_t\,dt$ should be linear with a slope of k^*_{relax}[ROH] and an intercept of $-(k_{reac} + k_{ex})$[ROH]. Figure 6 shows a plot of $([Cl]_t - [Cl]_0)/\int_0^t [Cl]_t\,dt$ versus $\int_0^t [Cl]_t\,dt/\int_0^t [Cl]_t\,dt$ derived from the data in Figure 4.

The time profile of Cl was calculated with rate constant values obtained by regression calculations of eq 10:

$$[Cl]_t = [Cl]_0 \exp\{-(k_{reac} + k_{ex})[ROH]t\} + k^*_{relax}[ROH]\int_0^t [Cl^*]_t \exp\{-k^*_{relax}[ROH](t - x)\}\,dx \quad (11)$$

The calculated time profile for $[Cl]_t$ using eq 11 is shown as the solid line in Figure 4. The observed time profile of Cl is well reproduced over the whole range of the delay time. The values of the chemical reaction rate constant k^*_{reac} for Cl* + C_2H_5OH were thus determined by subtracting k^*_{relax} from values of (k^*_{reac} + k^*_{relax}) which were obtained from the single-exponential-decay profiles of the Cl*. Figure 7 shows a plot of the rates $k^*_{reac}[C_2H_5OH]$, $k^*_{relax}[C_2H_5OH]$, and (k^*_{reac} + k^*_{relax})$[C_2H_5OH]$ versus the C_2H_5OH concentration as determined by the analysis of time profiles for Cl and Cl* using eqs 10 and 11. Linear-least-squares fits give $k^*_{relax} = (1.82 \pm 0.21) \times 10^{-10}$ cm^3 $molecule^{-1}$ s^{-1} and $k^*_{reac} = (6.4 \pm 1.7) \times 10^{-11}$ cm^3 $molecule^{-1}$ s^{-1} for the Cl* + C_2H_5OH system. Quoted errors are two standard deviations from the least-squares fits together with our estimate of systematic uncertainties in the

TABLE 3: Kinetic Data for Cl*($^2P_{1/2}$) Atoms Derived in the Present Work

reactant	$(k^*_{reac} + k^*_{relax})^a$	$k^*_{reac}{}^b$	$k^*_{relax}{}^c$	$k^*_{reac}/k_{reac}{}^d$	$k^*_{reac}/(k^*_{reac} + k^*_{relax})^e$
CH_3OH	19.5 ± 1.3	3.5 ± 1.5	16.0 ± 1.5	0.65 ± 0.29	0.18 ± 0.08
C_2H_5OH	24.8 ± 1.4	6.4 ± 1.7	18.2 ± 2.1	0.67 ± 0.19	0.26 ± 0.07
n-C_3H_7OH	31.3 ± 1.8	10.7 ± 2.9	20.6 ± 4.0	0.62 ± 0.18	0.34 ± 0.10
i-C_3H_7OH	28.4 ± 1.6	8.5 ± 2.5	20.0 ± 2.6	0.93 ± 0.29	0.30 ± 0.09

[a] Rate constant for total removal (reaction + relaxation) of Cl* in units of 10^{-11} cm^3 molecule^{-1} s^{-1}. [b] Rate constant for loss of Cl* via reaction in units of 10^{-11} cm^3 molecule^{-1} s^{-1}. [c] Rate constant for loss of Cl* via relaxation in units of 10^{-11} cm^3 molecule^{-1} s^{-1}. [d] Ratio of Cl*($^2P_{1/2}$) (channel 3) to Cl($^2P_{3/2}$) (channel 1) reactivity. [e] Fraction of Cl*($^2P_{1/2}$) loss occurring via reaction.

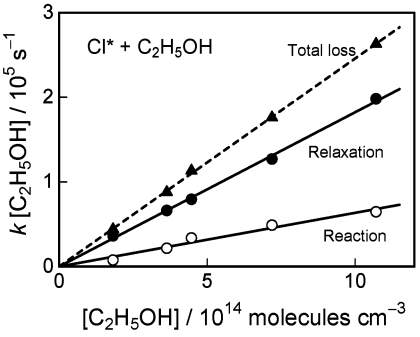

Figure 7. Pseudo-first-order relaxation and reaction rates of Cl* atoms versus C_2H_5OH partial pressure: filled triangles, total loss rate $(k^*_{reac} + k^*_{relax})$[ROH]; filled circles, relaxation rate k^*_{relax}[ROH]; and open circles, reaction rate k^*_{reac}[ROH].

reactant concentration measurements. Similar experiments and analyses were performed using CH_3OH, n-C_3H_7OH, and i-C_3H_7-OH reactants. The k^*_{reac} and k^*_{relax} values obtained are listed in Table 3, together with relative importance of channels 1, 3, and 4.

We also analyzed temporal behavior of Cl using a Runge−Kutta method as reported by Hitsuda et al.[15,31] The simultaneous differential equations, (7) and (8), were solved numerically to obtain the temporal behavior of Cl. The detailed balance principle was assumed between the excitation and relaxation rate constants, k_{ex} and k^*_{relax}. The k^*_{reac} and k^*_{relax} values obtained by the Runge−Kutta method were in good agreement with those by the integral profiles method.

4. Discussion

4.1. Reaction of Cl($^2P_{3/2}$) Atoms with CH_3OH, C_2H_5OH, n-C_3H_7OH, and i-C_3H_7OH. The room-temperature rate constants for Cl + ROH reactions determined using the VUV-LIF technique in the present study are listed in Table 2. Literature data obtained using a variety of experimental techniques are also given in Table 2 for comparison. The present study is the first to apply the VUV-LIF technique. The rate constant determined for Cl + CH_3OH in this study is in agreement with those from previous studies[8,10,11,22,25] within the combined experimental uncertainties. Our data for reactions of Cl with C_2H_5OH, n-C_3H_7OH, and i-C_3H_7OH are, within the quoted uncertainties, in good agreement with the NASA/JPL and IUPAC recommendations and most previous experimental studies. It should be noted that this is a first report to apply an absolute technique for determination of the rate constants for n-C_3H_7OH and i-C_3H_7OH reactions (Table 2).

As listed in Table 2, the reactivity of Cl toward alcohols increases along the series CH_3OH, C_2H_5OH, and n-C_3H_7OH. This observation presumably reflects a relative change in activation energy for H-atom abstraction along the series. The height of the activation barrier should be related to the exothermicity of the reaction channels. At room temperature, the H-atom abstraction channels from the α-, β-, and γ-positions are exothermic, while those from the hydroxyl position are slightly endothermic as listed in Table 1.

In the Cl + CH_3OH reaction, it has been suggested that H-atom abstraction occurs predominantly (>95%) from the α-position forming the CH_2OH radical rather than CH_3O radical.[23,32−34] Rudić et al.[23] performed ab initio calculations to estimate the energetics for H-atom abstraction from the α-position and hydroxyl position for Cl + CH_3OH reaction at the G2//MP2/6-311G(d,p) level of theory. They revealed that α-hydrogen abstraction has no intrinsic barrier, while hydrogen abstraction from the hydroxyl group has an energy barrier of 8.27 kcal mol^{-1} relative to the reactants.

Similarly, reaction of Cl with C_2H_5OH proceeds predominantly (>90%) via H-atom abstraction from the α-position.[5,6,33,35] Ab initio calculations for Cl + C_2H_5OH reaction[23] suggest that α-hydrogen abstraction has no intrinsic barrier while β-hydrogen and hydroxyl hydrogen abstraction have energy barriers of 0.73 and 8.53 kcal mol^{-1} relative to the reactants, respectively (see Figure 1). For the Cl + n-C_3H_7OH reaction, it has been suggested that H atoms at both the α- and β-positions are abstracted.[6] The trend k_{reac}(Cl($^2P_{3/2}$) + CH_3OH) < k_{reac}-(Cl($^2P_{3/2}$) + C_2H_5OH) ≈ k_{reac}(Cl($^2P_{3/2}$)+i-C_3H_7OH) < k_{reac}(Cl-($^2P_{3/2}$)+n-C_3H_7OH) follows the trend of exothermicity values listed in Table 1 for H-atom abstraction from the α-position; that is, ΔH_α(Cl+CH_3OH) > ΔH_α(Cl+C_2H_5OH) ≈ ΔH_α(Cl+i-C_3H_7OH) > ΔH_α(Cl+n-C_3H_7OH).

4.2. Chemical Reaction of Cl*($^2P_{1/2}$) Atoms with CH_3OH, C_2H_5OH, n-C_3H_7OH, and i-C_3H_7OH. As indicated in Table 3, chemical reaction accounts for 18−34% of the total removal of Cl* in collisions with CH_3OH, C_2H_5OH, n-C_3H_7OH, and i-C_3H_7OH. This result is consistent with previous reports that chemical reaction is of minor importance as a removal mechanism of Cl* in collisions with CH_4, C_2H_6, C_3H_8, n-C_4H_{10}, and i-C_4H_{10}.[14,15,31,36]

Interestingly, in the reaction of Cl + C_2H_5OH, the barrier for H-atom abstraction from the β-position (0.73 kcal mol^{-1} with respect to the reactants[23]) is lower than the Cl* spin−orbit excitation. If spin−orbit excitation were effective in overcoming the barrier for H-atom abstraction from the β-position, we would expect that Cl* atoms would have a greater reactivity than Cl. However, our results indicate that Cl* is less reactive than Cl toward C_2H_5OH at room temperature (k^*_{reac}/k_{reac} = 0.67; see Table 3). We also find that Cl* atoms have lower reactivity than Cl atoms in reactions with CH_3OH, n-C_3H_7OH, and i-C_3H_7OH (k^*_{reac}/k_{reac} = 0.65, 0.62, and 0.93, respectively).

Hitsuda et al.[15,31] reported $k^*_{reac}/k_{reac} \approx 0.3$ for C_3H_8, n-C_4H_{10}, and i-C_4H_{10}, and $k^*_{reac}/k_{reac} < 0.17$ for C_2H_6 and C_3D_8, and attributed the lower reactivity of Cl* to adiabatic correlations between the reactant state and the product state. The reactant state of Cl($^2P_{3/2}$) + R−H $^1\Sigma^+(^1A')$ correlates adiabatically to the product state HCl($X^1\Sigma^+$) + R• due to the $^2\Sigma^+(^2A')$ symmetry in the $C_{\infty v}$ (C_s) point group, while Cl*($^2P_{1/2}$) + R−H $^1\Sigma^+(^1A')$ correlates to the highly excited product state HCl($^1\Sigma^+$) + R•*

due to the $^2\Pi_{1/2}(^2A')$ symmetry. The reaction of $Cl^*(^2P_{1/2})$ with R−H to produce $HCl(X^1\Sigma^+)$ + R• should take place through nonadiabatic couplings of the two surfaces. Results from the present study show that Cl* is less reactive than Cl toward ROH at room temperature. These results imply that the adiabatically forbidden character between the potential energy surfaces is effective for Cl*/Cl + ROH reactions.

The k^*_{reac} value for Cl*-atom reactions with ROH combined with the population of the excited state (0.71% at 298 K) leads to the conclusion that Cl* atoms are responsible for 0.5%, 0.5%, 0.4%, and 0.7% of the observed reactivity of thermalized chlorine atoms with CH_3OH, C_2H_5OH, *n*-C_3H_7OH, and *i*-C_3H_7-OH, respectively.

4.3. Relaxation of $Cl^*(^2P_{1/2})$ Atoms in Collisions with CH_3OH, C_2H_5OH, *n*-C_3H_7OH, and *i*-C_3H_7OH. The rate constants for relaxation (channel 4) of Cl*, k^*_{relax}, in collisions with CH_3OH, C_2H_5OH, *n*-C_3H_7OH, and *i*-C_3H_7OH are listed in Table 3. Hitsuda et al.[15,31] and Matsumi et al.[14] have measured rate constants for relaxation of Cl* by several hydrocarbons using the VUV-LIF technique. Chichinin[26] measured the relaxation rate constants of Cl* with a series of inorganic and organic molecules using time-resolved laser magnetic resonance (LMR) and suggested that electronic−vibrational (E−V) energy exchange is the dominant pathway for Cl* relaxation.[26] For hydrocarbons, the relaxation rate constants of Cl* increase as follows: CH_4, 2.7×10^{-11} cm^3 molecule^{-1} s^{-1}; C_2H_6, 1.12×10^{-10} cm^3 molecule^{-1} s^{-1}; and C_3H_8, 1.29×10^{-10} cm^3 molecule^{-1} s^{-1}.[15,16,26,27,31] Interestingly, the present study shows that rate constants for relaxation of Cl* by CH_3OH, C_2H_5OH, *n*-C_3H_7OH, and *i*-C_3H_7OH are a factor of approximately 2−6 times larger than those for the corresponding alkanes (CH_4, C_2H_6, and C_3H_8). This may be explained by the existence of C−O stretching mode in alcohols. According to the NIST Chemistry WebBook,[12] the fundamental vibrational frequencies of O−H, C−H, and C−O stretching modes in alcohols are about 3700, 3000, and 1000 cm^{-1}, respectively. The C−O stretching mode in alcohols has a very strong band intensity,[12] and its fundamental vibrational frequency is close to the spin−orbit energy difference between Cl* and Cl (882 cm^{-1}). It seems likely that the near resonance between the C−O stretching frequency and the spin−orbit excitation energy accounts for the efficiency with which collisions with alcohol molecules relax Cl*.

5. Conclusion

The kinetics of reactions of Cl and Cl* atoms with CH_3OH, C_2H_5OH, *n*-C_3H_7OH, and *i*-C_3H_7OH were studied at 295 K. VUV-LIF combined with laser flash photolysis techniques enabled independent monitoring of the temporal behaviors of both spin−orbit states of chlorine atoms. The kinetic data measured here for reactions of spin−orbit ground Cl atoms with the alcohols were consistent with results from previous studies. The reactivity of spin−orbit excited Cl* atoms toward alcohols was examined for the first time. Rate constants for chemical reaction of Cl* atoms with alcohols are smaller than those for the corresponding reactions involving Cl atoms. The majority of collisions between Cl* and alcohol molecules lead to relaxation of Cl* to Cl. Under ambient conditions spin−orbit excited Cl* atoms are responsible for 0.5%, 0.5%, 0.4%, and 0.7% of the observed reactivity of thermalized chlorine atoms toward CH_3OH, C_2H_5OH, *n*-C_3H_7OH, and *i*-C_3H_7OH.

Acknowledgment. This work was partly supported by Grants-in-Aid from the Ministry of Education, Culture, Sports, Science and Technology, of Japan. The research grant for Dynamics of the Sun-Earth-Life Interactive System, No.G-4, the 21st Century COE Program from the Ministry, is also acknowledged. This work was also supported in part by the Mitsubishi Chemical Corporation Fund (K.T.) and the Steel Industrial Foundation for the Advancement of Environmental Protection Technology (Y.M).

References and Notes

(1) Finlayson-Pitts, B. J.; Pitts, J. N. *Chemistry of the Upper and Lower Atmosphere: Theory, Experiments and Applications*; Academic Press: San Diego, CA, 2000.
(2) Dobe, S.; Otting, M.; Temps, F.; Wagner, H. G.; Ziemer, H. *Ber. Bunsen-Ges. Phys. Chem.* **1993**, *97*, 877.
(3) Wallington, T. J.; Skewes, L. M.; Siegl, W. O.; Wu, C.-H.; Japar, S. M. *Int. J. Chem. Kinet.* **1988**, *20*, 867.
(4) Nelson, L.; Rattigan, O.; Neavyn, R.; Sidebottom, H.; Treacy, J.; Nielsen, O. J. *Int. J. Chem. Kinet.* **1990**, *22*, 1111.
(5) Taatjes, C. A.; Christensen, L. K.; Hurley, M. D.; Wallington, T. J. *J. Phys. Chem. A* **1999**, *103*, 9805.
(6) Khatoon, T.; Edelbuttel, J.; Hoyermann, K.; Wagner, H. Gg. *Ber. Bunsen-Ges. Phys. Chem.* **1989**, *93*, 626.
(7) Crawford, M. A.; Li, Z.; Heuerman, H. A.; Kinscherff, D. *Int. J. Chem. Kinet.* **2004**, *36*, 584.
(8) Seakins, P. W.; Orlando, J. J.; Tyndall, G. S. *Phys. Chem. Chem. Phys.* **2004**, *6*, 2224.
(9) Michael, J. V.; Nava, D. F.; Payne, W. A.; Stief, L. J. *J. Chem. Phys.* **1979**, *70*, 3652.
(10) Tyndall, G. S.; Orlando, J. J.; Kegley-Owen, C. S.; Wallington, T. J.; Hurley, M. D. *Int. J. Chem. Kinet.* **1999**, *31*, 776.
(11) Smith, J. D.; DeSain, J. D.; Taatjes, C. A. *Chem. Phys. Lett.* **2002**, *366*, 417.
(12) *National Institute of Standards and Technology Chemical Kinetics Database*; NIST: Gaithersburg, MD, 1998; Vol. 17.
(13) Dagdigian, P. J.; Campbell, M. L. *Chem. Rev.* **1987**, *87*, 1.
(14) Matsumi, Y.; Izumi, K.; Skorokhodov, V.; Kawasaki, M.; Tanaka, N. *J. Phys. Chem. A* **1997**, *101*, 1216.
(15) Hitsuda, K.; Takahashi, K.; Matsumi, Y.; Wallington, T. J. *J. Phys. Chem. A* **2001**, *105*, 5131.
(16) Chichinin, A. I.; Krasnoperov, L. N. *Chem. Phys. Lett.* **1986**, *124*, 8−13.
(17) McMillen, D. F.; Golden, D. M. *Annu. Rev. Phys. Chem.* **1982**, *33*, 493.
(18) Holmes, J. L.; Lossing, F. P.; Mayer, P. M. *J. Am. Chem. Soc.* **1991**, *113*, 9727.
(19) Block, D. A.; Armstrong, D. A.; Rauk, A. *J. Phys. Chem. A* **1999**, *103*, 3562.
(20) Luo, N.; Kombo, D. C.; Osman, R. *J. Phys. Chem. A* **1997**, *101*, 926.
(21) Zhou, W.; Yuan, Y.; Zhang, J. *J. Chem. Phys.* **2003**, *119*, 7179.
(22) Atkinson, R.; Baulch, D. L.; Cox, R. A.; Hampson, R. F., Jr.; Kerr, J. A.; Rossi, M. J.; Troe, J. *J. Phys. Chem. Ref. Data* **1997**, *26*, 521−1011.
(23) Rudić, S.; Murray, C.; Ascenzi, D.; Anderson, H.; Harvey, J. N.; Orr-Ewing, A. J. *J. Chem. Phys.* **2002**, *117*, 5692.
(24) Zhang, J.; Dulligan, M.; Wittig, C. *J. Chem. Phys.* **1997**, *107*, 1403.
(25) Sander, S. P.; Friedl, R. R.; Golden, D. M.; Kurylo, M. J.; Huie, R. E.; Orkin, V. L.; Moortgat, G. K.; Ravishankara, A. R.; Kolb, C. E.; Molina, M. J.; Finlayson-Pitts, B. J. *Chemical Kinetics and Photochemical Data for Atmospheric Studies*; JPL Publication 02-25; JPL: Pasadena, CA, 2003.
(26) Chichinin, A. I. *J. Chem. Phys.* **2000**, *112*, 3772−3779.
(27) Tyndall, G. S.; Orlando, J. J.; Kegley-Owen, C. S. *J. Chem. Soc., Faraday Trans.* **1995**, *91*, 3055.
(28) Yamasaki, K.; Taketani, F.; Sugiura, K.; Tokue, I.; Tsuchiya, K. *J. Phys. Chem. A* **2004**, *108*, 2382.
(29) Yamasaki, K.; Taketani, F.; Tomita, S.; Sugiura, K.; Tokue, I. *J. Phys. Chem. A* **2003**, *107*, 2442.
(30) Yamasaki, K.; Watanabe, A.; Kakuda, T.; Tokue, I. *Int. J. Chem. Kinet.* **1998**, *30*, 47.
(31) Hitsuda, K.; Takahashi, K.; Matsumi, Y.; Wallington, T. J. *Chem. Phys. Lett.* **2001**, *346*, 16.
(32) Bechtel, H. A.; Camden, J. P.; Zare, R. N. *J. Chem. Phys.* **2004**, *120*, 4231.
(33) Ohta, T.; Bandow, H.; Akimoto, H. *Int. J. Chem. Kinet.* **1982**, *14*, 173.
(34) Payne, W. A.; Brunning, J.; Mitchell, M. B.; Stief, L. J. *Int. J. Chem. Kinet.* **1988**, *20*, 63.
(35) Meier, U.; Grotheer, H. H.; Riekert, G.; Just, T. *Chem. Phys. Lett.* **1985**, *115*, 221.
(36) Zhou, J.; Lin, J. J.; Zhang, B.; Liu, K. *J. Phys. Chem. A* **2004**, *108*, 7832.